Research Article

Journal of PeptideScience

Received: 7 December 2011 Revised: 6 July 2012 Accepted: 9 July 2012 Published online in Wiley Online Library: 1 August 2012

(wileyonlinelibrary.com) DOI 10.1002/psc.2439

Synthesis and properties of cyclic gomesin and analogues

Alessandra Machado,[a,d] Marcos A. Fázio,[b,e] Antonio Miranda,[b] Sirlei Daffre[c] and M. Teresa Machini[a]*

Gomesin (*Gm*) was the first antimicrobial peptide (AMP) isolated from the hemocytes of a spider, the Brazilian mygalomorph *Acanthoscurria gomesiana*. We have been studying the properties of this interesting AMP, which also displays anticancer, antimalarial, anticryptococcal and anti-*Leishmania* activities. In the present study, the total syntheses of backbone-cyclized analogues of *Gm* (two disulfide bonds), [Cys(Acm)^{2,15}]-*Gm* (one disulfide bond) and [Thr^{2,6,11,15},D-Pro^{9}]-*Gm* (no disulfide bonds) were accomplished, and the impact of cyclization on their properties was examined. The consequence of simultaneous deletion of pGlu^{1} and Arg^{16}-Glu-Arg^{18}-NH$_2$ on *Gm* antimicrobial activity and structure was also analyzed. The results obtained showed that the synthetic route that includes peptide backbone cyclization on resin was advantageous and that a combination of 20% DMSO/NMP, EDC/HOBt, 60 °C and conventional heating appears to be particularly suitable for backbone cyclization of bioactive peptides. The biological properties of the *Gm* analogues clearly revealed that the N-terminal amino acid pGlu^{1} and the amidated C-terminal tripeptide Arg^{16}-Glu-Arg^{18}-NH$_2$ play a major role in the interaction of *Gm* with the target membranes. Moreover, backbone cyclization practically did not affect the stability of the peptides in human serum; it also did not affect or enhanced hemolytic activity, but induced selectivity and, in some cases, discrete enhancements of antimicrobial activity and salt tolerance. Because of its high therapeutic index, easy synthesis and lower cost, the [Thr^{2,6,11,15},D-Pro^{9}]-*Gm* analogue remains the best active *Gm*-derived AMP developed so far; nevertheless, its elevated instability in human serum may limit its therapeutic potential. Copyright © 2012 European Peptide Society and John Wiley & Sons, Ltd.

Keywords: antimicrobial peptide; head-to-tail cyclization; peptide truncation; high temperatures

Introduction

The spread of bacterial resistance, a major concern in contemporary medicine, has spurred demand for novel antibiotics [1]. In such circumstances, peptides with antimicrobial activity (AMPs) are considered potential candidates or templates for the design of highly active low-molecular-mass compounds.

The group of known AMPs, somewhat large, includes naturally occurring peptides and *de novo* designed synthetics (http://bbcm1.univ.trieste.it/~tossi/pag1.htm, http://www.cryst.bbk.ac.uk/peptaibol/home.shtml, http://oma.terkko.helsinki.fi:8080/~SAPD) that are able to: (i) inhibit the growth or kill Gram-positive and Gram-negative bacteria, fungi and/or protozoa at very low concentrations [2,3]; (ii) inhibit replication of enveloped viruses such as influenza A virus [4], vesicular stomatitis virus [5] and human immunodeficiency virus (HIV-1) [6]; (iii) display anticancer activity [7,8]; and (iv) promote wound healing [9]. The naturally occurring AMPs are components of the innate immunity system found in almost all species of life [10,11].

The lengths, sequences and structures of AMPs vary significantly as they are short-sized, medium-sized or large molecules, present high content of specific amino acids (glycine, proline, trypophan or positively charged amino acids), contain N-terminus and/or C-terminus free or modified, are linear or conformationally restricted (because of backbone cyclization or presence of intramolecular disulfide bridges) and adopt α-helical, β-hairpin-like or β-sheet structures as well as a combination of β-sheet and α-helical structures. Most of the known AMPs are cationic and exhibit an amphipatic spatial arrangement, with opposing hydrophobic and positively charged faces, when in contact with the target membrane [12,13].

Gomesin (*Gm*) was the first AMP isolated from the hemocytes of a spider, the mygalomorph *Acanthoscurria gomesiana*. This peptide is active against Gram-positive and Gram-negative bacteria, fungi and eukaryotic parasites; it consists of 18 amino acid residues, presents two disulfide bridges (linking Cys^{2} to Cys^{15} and Cys^{6} to Cys^{11}) and carries two post-translational modifications: cyclization of the N-terminal glutamic acid into pyroglutamic acid, pGlu^{1} and

* *Correspondence to: M. Teresa Machini (Miranda, M.T.M), Department of Biochemistry, Institute of Chemistry, University of São Paulo, PO Box. 26077, 05513-970, São Paulo, SP, Brazil. E-mail: mtmachini@iq.usp.br*

Preliminary accounts of certain aspects of this work were described as a communication in Machado, A., Fázio, M. A., Miranda, A.; Daffre, S. & Miranda, M.T.M., Synthesis of conformationally constrained head-to-tail cyclic gomesin. E. Benedetti & C. Pedone (Eds.), In Peptides 2002 (Proc. 27th. Eur. Pept. Symp.), Benedetti, E. & Pedone, C. (Eds.), Edizione Ziino: Napoli, Italy, 2002, 224–225. Abstract in *J. Pept. Sci*., 2002; **8**: S88 (P-A44).

a *Department of Biochemistry, Institute of Chemistry, University of São Paulo, São Paulo, Brazil*

b *Department of Biophysics, Federal University of São Paulo, São Paulo, Brazil*

c *Department of Parasitology, Institute of Biomedical Sciences, University of São Paulo, São Paulo, Brazil*

d *Federal University of Technology of Paraná, Francisco Beltrão, PR, Brazil*

e *Mackenzie Presbyterian University, São Paulo, SP, Brazil*

Journal of PeptideScience

amidation of the C-terminal arginine, Arg^{18}-NH_2 (Figure 1). Sequence alignments suggested strong similarities between *Gm* and tachyplesins, polyphemusin, androctonin and protegrins [14]. Despite a limited cytotoxic effect on human erythrocytes, its broad activity spectrum [15–17] and high potency render *Gm* likely to be used in therapeutics or as a guide for the design of new drugs. Therefore, the structural properties of *Gm* have become a relevant issue [18].

In 2002, Mandard and coworkers reported that the global fold of this antimicrobial peptide in solution consists of a well-resolved two-stranded antiparallel β-sheet connected by a noncanonical β-turn, confirming that the distribution of its hydrophobic and hydrophilic amino acid residues was identical to that observed in protegrin-1 and androctonin [19]. This important information prompted us to investigate the structure–activity relationship of *Gm*. At first, we studied the importance of the two disulfide bridges for its bioactivities, conformation and serum stability by synthesizing and analyzing linearized, monocyclic disulfide-bridged analogues (including [$Cys(Acm)^{2,15}$]-*Gm*) and bicyclic side-chain lactam-bridged analogues. The results led us to conclude that (i) as with most AMPs, the antimicrobial and hemolytic activities of *Gm* are correlated events; (ii) at least one disulfide bridge is required for satisfactory antimicrobial activity; (iii) both bridges are required for full antimicrobial activity and high serum stability [20]. Next, we conceived, synthesized and tested a new linearized form of *Gm* whose cysteines were replaced by threonines and glutamine[9] by D-Pro: [$Thr^{2,6,11,1}$,D-Pro^{9}]-*Gm*. Besides being easy to prepare in good quality and reasonable yields, this analogue was equipotent to *Gm* against *Candida albicans*, slightly less active against *Micrococcus luteus* (twofold) and *Escherichia coli* (fourfold) and 2.5-fold less hemolytic. As a result, its therapeutic index (TI) was 32-fold higher than that of *Gm* [21].

In this paper, we report the total synthesis of backbone-cyclized analogues of *Gm* with two disulfide bonds, [$Cys(Acm)^{2,15}$]-*Gm* with one disulfide bond and [$Thr^{2,6,11,1}$,D-Pro^{9}]-*Gm*, a linearized analogue, and the effect of such conformational constraints on antimicrobial and hemolytic activity, salt tolerance and serum stability. We also report the consequence of simultaneous deletion of $pGlu^{1}$ and Arg^{16}-Glu-Arg^{18}-NH_2 on *Gm* antimicrobial activity and structure. To perform such a study, we took into account that (i) antibiotics of high TIs are more selective [22]; (ii) antifungal activities of *Gm* and [$Thr^{2,6,11,15}$,D-Pro^{9}]-*Gm* are affected under high salt conditions; (iii) backbone cyclization of linear AMPs [23,24] and of AMPs structurally related to *Gm* [25] has provided less toxic or salt-sensitive active analogues [26,27]; (iv) the synthesis of a backbone-cyclized peptide containing two disulfide bridges could be a challenging synthetic task, therefore, a topic of interest for peptide chemists [23,28]; (v) our group has already succeeded in preparing different peptides with the help of customized protocols at 60 °C by using conventional heating [29–31]; (vi) *E. coli*, *S. aureus* and *C. albicans* are microorganisms of substantial scientific interest and clinical importance.

Experimental Section

Stepwise Solid-Phase Peptide Synthesis

Synthetic *Gm*, [$Cys(Acm)^{2,15}$]-*Gm* and [$Thr^{2,6,11,15}$,D-Pro^{9}]-*Gm* were previously obtained in our laboratories (Table 1) [20,21]. The novel *Gm* analogues (Table 1) were synthesized manually by the solid-phase method at room temperature by using the *tert*-butyloxycarbonyl (Boc) chemistry and our previously optimized protocols [29–32].

The side-chain protecting groups used were Tos (for Arg), Bzl (for Thr and Tyr), 2-Cl-Z (for Lys), Acm (for Cys^{2} and Cys^{15}) and 4-Meb (for Cys^{6} and Cys^{11}, but in the case of c(1–18)[Gln^{1}]-*Gm* and c(1–18)[Gln^{1},$Cys(Acm)^{2,15}$]-*Gm* 4-Meb was also employed for Cys^{2} and Cys^{15}. The resins employed were 4-methylbenzhydrylamine resin (MBHA resin from Advanced ChemTech, Louisville, KY; substitution level of 0.67 mmol/g), 0.5 g for the synthesis of *Gm*(2–15); Boc-Arg(Tos)-4-hydroxymethyl-phenylacetamidomethyl (PAM resin from Bachem California, Torrance, CA; aminoacylation level of 0.60 mmol/g), 1.3 g for the synthesis of c(1–18)[Gln^{1},$Cys(Acm)^{2,15}$]-*Gm*). The Boc-Glu(MBHA resin)-OFm was prepared in our laboratory as described later (0.5 and 1.0 g for the syntheses of c(1–18)[Gln^{1}]-*Gm* and c(1–18)[Gln^{1},$Thr^{2,6,11,15}$,D-Pro^{9}]-*Gm*, respectively).

Progression of aminoacylation of the resin and all reactions required for peptide assembly on it (couplings/recouplings, deprotections and acetylations) were monitored by collecting a sample of the washed resin, amino acid resin or peptide resin and submitting it to the ninhydrin test [33]. As in our previous

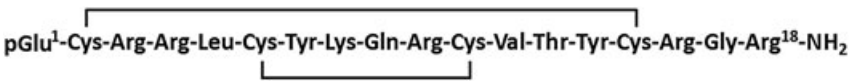

Figure 1. Amino acid sequence with side-chain S–S bridges of gomesin (*Gm*).

Table 1. Amino acid sequences and mass spectrometry data of the peptides synthesized and tested

Peptide	Purification yield/Peptide purity (%)	$[MH]^+$ calcd./found	Peptide content (%)
Gm	—[a]	2270.4 (2270.0)[a]	67
Gm(2–15)	7/95	1790.0 (1790.2)	65
c(1–18)[Gln^{1}]-*Gm*	<1/98	2271.8 (2271.0)	64
[$Cys(Acm)^{2,15}$]-*Gm*	—[a]	2414.0 (2415.0)[a]	80
c(1–18)[Gln^{1},$Cys(Acm)^{2,15}$]-*Gm*	4.7/98	2414.9 (2414.2)	67
[$Thr^{2,6,11,15}$, D-Pro^{9}]-*Gm*	—[a]	2235.5 (2236.5)[a]	66
c(1–18)[Gln^{1}, $Thr^{2,6,11,15}$, D-Pro^{9}]*Gm*	26/98	2234.6 (2234.8)	68

[a]Previously synthesized in our laboratories [20,21].

studies [29–31], the reactions at room temperature were carried out for 60 min in glass-fritted reaction vessels under shaking, whereas those performed at 60 °C using conventional heating took place for 30 min in water-jacketed glass-fritted vessels connected to a heated water-bath circulator (Polyscience 8001; temperature variation of only 1 °C), under shaking.

Boc-Glu(MBHA resin)-OFm was obtained by reacting for 1 h at room temperature MBHA resin (Advanced ChemTech, substitution of 0.67 mmol/g) with Boc-Glu-OFm (2.5-fold excess) in the presence of equimolar amount of *N*,*N*′-diisopropylcarbodiimide (DIC)/1-hydroxybenzotriazole (HOBt) (1 : 1, mol/mol) in dichloromethane (DCM). After filtration and alternating washings with DMF, MeOH and DCM, the resulting aminoacylated resin provided a negative ninhydrin test [33].

Coupling of Boc–amino acid (2.5-fold excess) to the resin or growing peptide resin was carried out for 60 min in DCM containing equimolar amounts DIC/HOBt (1 : 1, mol/mol) or in DMF containing *O*-benzotriazol-1-yl-*N*,*N*,*N*′,*N*′-tetramethyluronium tetrafluoroborate (TBTU) and diisopropylethylamine (DIPEA) at apparent pH 8.0. The reaction medium was removed by filtration. The peptide resin was washed with DMF, MeOH and DCM prior to the ninhydrin test [33]. When the coupling was not complete, Boc–amino acid recoupling was carried out. Post-recoupling washes were performed as described for the post-coupling washes.

Boc group (used to protect the α-amino group of the N-terminal amino acid residue of the resin-linked peptides) removal was performed in 50% trifluoroacetic acid (TFA)/DCM for 20 min. After sequential washes of the peptide resin with DCM, MeOH and 5% DIPEA/DCM, the presence of free amino groups was indicated by a positive ninhydrin test [33].

The amounts of the side-chain protected peptide resins obtained were 1.45 g of *Gm*(2–15)-MBHA, 3.66 g of [Gln^{1},Cys(Acm)^{2,15}]-*Gm*-PAM, 0.52 g of [Gln^{1},Thr^{2,6,11,15},D-Pro^{9}]-*Gm*-MBHA, 1.5 g of [Glu(MBHA resin)^{9}-OFm]-*Gm* and 2.84 g of [Glu(MBHA resin)^{1}-OFm,Thr^{2,6,11,15},D-Pro^{9}]-*Gm*.

Backbone Cyclization on Resin

[Glu(MBHA resin)^{9}-OFm]-*Gm* (0.2 g) and [Glu(MBHA resin)^{1}-OFm, Thr^{2,6,11,15},D-Pro^{9}]-*Gm* (0.3 g) had the Fm group removed in 20% piperidine/DMF containing anisole for 10 min to give the corresponding carboxyl-free side-chain protected peptide resins [Glu(MBHA resin)^{9}]-*Gm* and [Glu(MBHA resin)^{1},Thr^{2,6,11,15},D-Pro^{9}]-*Gm*. The experimental conditions used for backbone cyclizations to produce the corresponding resin-bound side-chain protected cyclized peptides c(1–18)[Gln^{1}]-*Gm* and c(1–18)[Gln^{1},Thr^{2,6,11,15},D-Pro^{9}]-*Gm* (Table 2) were inspired by those of previous related studies [34–36] , particularly by those employed for lactamization of corticotropin-releasing factor (CRF) analogues [37]. After alternating washes with the solvents mixtures employed and MeOH, the peptide resins were submitted to the Kaiser test [33] for monitoring the progression of the reaction. When the result was positive, the reaction was repeated under identical experimental conditions. When it was negative, the resulting peptide resins were filtered, and washed with NMP and MeOH.

The occurrence of backbone cyclization was also confirmed by peptide detachment from resin/full deprotection of a small amount of resulting peptide resin followed by analysis of the crude peptide by LC/ESI–MS and detection of the desired cyclic analogue in it.

Full Deprotection and Simultaneous Cleavage of the Peptide from Resin

A small fraction of each side-chain protected peptide resin obtained was exposed for 2 h to a mixture of condensed anhydrous hydrogen fluoride (HF) with anisole, *m*-cresol and dimethyl sulfide (DMS) [9 : 0.5 : 0.25 : 0.25 (v/v/v/v)]. The released peptide was precipitated in diisopropyl ether, extracted with 0.1% TFA/water or 60% acetonitrile (AcCN, chromatographic grade)/0.1% TFA and lyophilized. Identification of the desired analogue in the crude peptide obtained was carried out by analysis of the extract by LC/ESI–MS.

The amounts of crude peptides obtained were as follows: 69 mg of crude [Cys(Acm)^{2,15}]-*Gm*(2–15), 283 mg of [Gln^{1},Cys(Acm)^{2,15}]-*Gm*, 102 mg [Gln^{1},Thr^{2,6,11,15},D-Pro^{9}]-*Gm*, 143 mg of [Gln^{1}]-*Gm* and 262 mg of [Gln^{1},Thr^{2,6,11,15},D-Pro^{9}]-*Gm*. Purification by RP-HPLC was performed as described later. When required, disulfide bond formation was performed prior to purification.

Disulfide Bond Formation

Air oxidation reactions were performed by dissolving the reduced crude peptides in 10% AcCN/0.1% TFA at concentration of 0.2 mM and adjusting the pH of the resulting solutions to 8.0 with 10% ammonium hydroxide solution [20]. Monitoring was performed by analytical RP-HPLC on a Vydac C_{18} column (5 μm, 300 Å, 0.46 cm 25.0 cm) under the following conditions: 0.1% TFA/water as solvent A, 60% AcCN/0.1% TFA as solvent B, eluent flow rate of 10 ml/min and wavelength of 210 nm. Once the disulfide bonds were formed, the pH of the reaction media was adjusted to 4.0, and they were lyophilized.

Table 2. Head-to-tail cyclization of peptide resins

Coupling reagent	Solvent or mixture	Temperature	Time for negative ninhydrin test (h)
[Glu(MBHA resin)^{9}]-*Gm* ➔ c(1–18)[Glu(MBHA resin)^{9}]-*Gm*			
EDC HOBt	DMF	Room[a]	31
HOBt	20% DMSO/NMP	Room[a]	3
HOBt	20% DMSO/NMP	60 °C	1
HOAt	20% DMSO/NMP	60 °C	2
[Glu(MBHA resin)^{1},Thr^{2,6,11,15},D-Pro^{9}]-*Gm* ➔ c(1–18)[Glu(MBHA resin)^{1},Thr^{2,6,11,15},D-Pro^{9}]-*Gm*			
EDC HOBt	20% DMSO/NMP	Room[a]	2
HOBt	20% DMSO/NMP	60 °C	1

[a]From 25 to 28 °C.

In the case of *Gm*(2–15), its crude synthetic precursor [Cys(Acm)^{2,15}]-*Gm*(2–15) (69 mg) was submitted to air oxidation as described earlier to give Cys^{6},Cys^{11} disulfide linked [Cys(Acm)^{2,15}]-*Gm*(2–15), which was purified by RP-HPLC as described later. The amount obtained (8 mg) had the Acm groups removed, and the free cysteines were oxidized by incubation with TFA (1 μmol peptide/ml) containing anisole (19 : 1, v/v) and 0.6 μmol of Tl(III) at 4 °C for 40–43 h followed by peptide precipitation with cold ethyl ether and recovery by centrifugation. Peptide extraction with mixture of acetonitrile (AcCN)/0.1% TFA in water followed by lyophilization afforded the desired *Gm*(2–15).

Backbone Cyclization in Solution

Purification of crude [Gln^{1},Cys(Acm)^{2,15}]-*Gm* (283 mg) by RP-HPLC furnished 20 mg of [Gln^{1},Cys(Acm)^{2,15}]-*Gm* in the bis-thiol form, which was submitted to disulfide bond formation involving Cys6 and Cys11 according to the procedure described above. The resulting monodisulfide [Gln^{1},Cys(Acm)^{2,15}]-*Gm* and twofold excess of EDC/HOBt (1 : 1, mol/mol) were kept in 28 ml of DMSO under stirring at room temperature. The progress of the reaction was monitored by analytical RP-HPLC. After 26 h, [Gln^{1},Cys(Acm)^{2,15}]-*Gm* was fully converted into c(1–18)[Gln^{1},Cys(Acm)^{2,15}]-*Gm* as confirmed by LC/ESI–MS analysis of the reaction media. The solvent was then removed under vacuum, and the dry residue was loaded on a semi-preparative column for purification of the cyclic crude product by RP-HPLC.

Peptide Purification

Crude lyophilized peptides were purified by RP-HPLC [32,38] using the following conditions: (i) a preparative Vydac C_{18} column (5 μm, 300 Å, 2.2 cm × 25.0 cm; The Separation Group, Inc., Hesperia, CA) coupled to a Beckman System Gold semi-preparative equipment, 0.1% TFA/water as solvent A, AcCN/0.1% TFA as solvent B, eluent flow rate of 10 ml/min and wavelength of 220 nm; (ii) a semi-preparative Vydac C_{18} column (5 μm, 300 Å, 1.0 cm × 25.0 cm; The Separation Group, Inc.) coupled to an LDC HPLC system (Thermo Separation Products, San Jose, CA; composed of a ConstaMetric 3500 pump, a ConstaMetric 3200 pump, a 3100 model UV–VIS detector, a 7125 model Rheodyne injector and a 745B Waters integrator) with a flow rate of 3 ml/min and at wavelength of 210 nm using the solvents A and B cited above. (ii) a semi-preparative Vydac C_{18} column (5 μm, 300 Å, 1.0 cm × 25.0 cm; The Separation Group, Inc.) coupled to an LDC HPLC system (Thermo Separation Products, composed of a ConstaMetric 3500 pump, a ConstaMetric 3200 pump, a 3100 model UV–VIS detector, a 7125 model Rheodyne injector and a 745B Waters integrator) with a flow rate of 3 ml/min and at a wavelength of 210 nm using the solvents A and B cited above.

Purifications of c(1–18)[Gln^{1},Thr^{2,6,11,15},D-Pro^{9}]-*Gm*, c(1–18)[Gln^{1},Cys(Acm)^{2,15}]-*Gm*, c(1–18)[Gln^{1}]-*Gm* and *Gm*(2–15) required the following steps: Step 1, triethylammonium phosphate (TEAP), pH 2.25, as solvent A, 40% AcCN/TEAP as solvent B, linear gradient elution from 20% to 60% B {peptide c(1–18)[Gln^{1}]-*Gm*} or from 20% to 50% B {peptide c(1–18)[Gln^{1},Thr^{2,6,11,15},D-Pro^{9}]-*Gm*} or from 5% to 65% B {peptide c(1–18) [Gln^{1},Cys(Acm)^{2,15}]-*Gm*} or from 25% to 55% B [peptide *Gm*(2–15) in 90 min]; Step 2, 0.1% TFA/water as solvent A, 60% AcCN/0.1% TFA as solvent B, linear gradient elution from 20% to 60% B {peptide c(1–18)[Gln^{1}]-*Gm*} or from 20% to 50% B {peptide c(1–18)[Gln^{1},Thr^{2,6,11,15},D-Pro^{9}]-*Gm*} or from 5% to 65% B {peptide c(1–18)[Gln^{1},Cys(Acm)^{2,15}]-*Gm*} or from 25% to 55% B [peptide *Gm*(2–15)] in 90 min.

As shown in Table 1, because of the heterogeneity of the crude peptides, the purification yields varied from less than 1% (for the peptides containing disulfide bridges) to 26% (for those without them).

Chemical Characterization of the Purified Peptides

The peptide purities were higher than 95%. Their identities were confirmed by: (i) LC/ESI–MS on a Micromass Quatro II triple quadrupole instrument coupled with a Shimadzu RP-HPLC system VP Series equipped with LC-10AD pumps, a SDP-10-AV detector and a 7125 Rheodyne injector; (ii) amino acid analysis on a Beckman 7300 automated amino acid analyzer [38]. Therefore, the molar mass and peptide content of each purified peptide were determined prior to the biological assays and spectroscopic analyses (Table 1).

Antimicrobial Assays

The activities of the purified peptides against *C. albicans* (MDM8), *E. coli* SBS 363 and *S. aureus* ATCC6538 (obtained from the Microbiology Department Collection, Biomedical Sciences Institute of São Paulo, USP, Brazil) were determined using the liquid growth inhibition assay [39,40]. Briefly, 10 μl of the peptide solution was added to 90 μl of a suspension of a midlogarithmic phase culture of bacteria starting at $OD_{595\ nm}$ 0.001 in poor broth nutrient medium (PB: 1.0 g peptone in 100 ml of H_2O containing 86 mM NaCl at pH 7.4; 217 mOsM). In the case of the antifungal activity, the medium used was the poor dextrose broth (1/2 PDB: 1.2 g potato dextrose in 100 ml of H_2O at pH 5.0; 79 mOsM). Microbial growth was measured by monitoring the OD increase at 595 nm. The minimum inhibitory concentration (MIC) was determined following incubation at 30 °C for 18 h. The MIC was the lowest concentration of peptide, preventing visible antimicrobial growth.

Hemolytic Activity Assays

The hemolytic activity of the purified peptides was measured as described earlier [21,32] by using fresh human erythrocytes washed three times with PBS (10 mM Na_2HPO_4, 1.8 mM K_2HPO_4, pH 7.4, containing 140 mM NaCl and 2.7 mM KCl). Two times serial dilutions of the peptides from concentrations of 0.19 to 50 μM were incubated with a suspension of 0.4% erythrocytes in PBS. After 1 h at 37 °C, the test tubes were centrifuged at 300 *g* for 5 min at 5 °C. Fifty-microliter aliquots of the supernatants were transferred to 96-well plates, and hemolysis was monitored at 405 nm by using a microtiter plate reader. Negative and positive controls were prepared in PBS and in PBS supplemented with 0.1% SDS, respectively. The hemolysis percentages were calculated using the following equation: % hemolysis = [($A_{405\,nm}$ in the peptide solution − $A_{405\,nm}$ in PBS)/($A_{405\,nm}$ in 0.1% SDS − $A_{405\,nm}$ in PBS)] × 100. Three independent experiments were performed.

Serum Stability Assays

Briefly, 20 μl of an aqueous peptide stock solution (10 mg/ml) was added to 1 ml of 25% pooled non-heat-inactivated human serum

in PBS and incubated at 37 °C. Fifty-microliter aliquots were taken and added to 5 μl of pure TFA at different time intervals (0, 0.5, 1, 2, 4 and 6 h) and incubated at 5 °C for 15 min. Following incubation, the resulting mixtures were centrifuged at 300 *g* for 5 min. Twenty microliters of the supernatants was injected in an on-line LC/ESI–MS equipment. Elution was performed using a linear gradient of AcCN in acidified water from 3% to 57% for 30 min at a flow rate of 0.4 ml/min. Peptide consumption, followed by the area of the corresponding peak in the chromatogram, allowed for evaluating peptide stability in serum [21].

Circular Dicroism Measurements

The peptides were dissolved alternatively in water, in 50% TFE/water or in 50 mM SDS/water at pH 4.0 to obtain 20 μM solutions [21,32]. The spectra were acquired on a Jasco J-810 spectropolarimeter (JASCO International Co. Ltd., Tokyo, Japan) coupled to a Peltier Jasco PFD-425S system for temperature control. Eight scans over a wavelength range of 190–250 nm were taken using a 1-mm path length quartz rectangular cell at 20 °C. Following baseline correction, the measured ellipticity, θ (millidegrees), was converted to the molar mean residue ellipticity [θ] (deg cm^2 dmol^{-1}).

Results

Synthesis, Backbone Cyclization, Purification and Chemical Characterization of the Peptides Studied

Peptide assembly on resin using our customized protocols was straightforward. The subsequent steps required to obtain the cyclic analogues (Figures 3 and 4) led to very small amounts of crude peptides. All of them showed contaminants removed during the purification steps, whose identification by LC/ESI–MS associated them to secondary reactions typical of solid-phase peptide synthesis, such as amino acid deletion, tyrosine ring alkylation, partial removal of Acm protecting group and peptide oligomerization.

Backbone cyclization performed conventionally (in solution and at room temperature) of [Gln^1,Cys(Acm)^{2,15}]-*Gm* to give c(1–18)[Gln^1,Cys(Acm)^{2,15}]-*Gm* required 26 h to complete. As shown in Table 2, backbone cyclization of [Glu(MBHA resin)^9]-*Gm* on resin at room temperature in DMF containing EDC/HOBt required 31 h, but replacement of DMF by 20% DMSO/NMP significantly enhanced the reaction rate (only 3 h to complete). In such binary mixture at 60 °C, the reaction was even faster, requiring only 1 h to complete. Replacement of HOBt by HOAt slowed it down (2 h to complete). At 60 °C and in the presence of EDC/HOBt in 20% DMSO/NMP, Glu(MBHA resin)^1,[Thr^{2,6,11,15},D-Pro^9]-*Gm* was converted into c(1–18)[Glu(MBHA resin)^1,Thr^{2,6,11,15},D-Pro^9]-*Gm* twofold faster than at room temperature. In fact, the analyses of the crude peptides by LC/ESI–MS confirmed that they contained the desired cyclic analogues as major components.

Antimicrobial Assays

Table 3 shows the growth-inhibiting MICs found for the final peptides against *E. coli* SBS 363, *S. aureus* ATCC6538 and *C. albicans* MDM8 at low (86 mM NaCl) and physiological (137 mM NaCl) salt concentrations.

At a low salt concentration, simultaneous deletion of the N-terminal pGlu^1 and of the amidated C-terminal tripeptide (Arg^{16}-Gly-Arg^{18}-NH$_2$) caused drastic decrease of activity (four to eight times) against the bacteria tested. The effect was less significant against the fungus *C. albicans*. Lack of one or two disulfides bridges showed to have also a strong negative effect on antimicrobial activity, corroborating our previous report that the substitution of the four cysteines by threonines with simultaneous replacement of Gln^9 by D-Pro^9 led to an analogue less active against the bacteria, but not against the fungus tested. Replacement of pGlu^1 by Gln^1 and subsequent backbone cyclization to give c(1–18)[Gln^1]-*Gm*, c(1–18)[Gln^1,Cys(Acm)^{2,15}]-*Gm* and c(1–18)[Thr^{2,6,11,15},D-Pro^9]-*Gm* led to the preservation or discrete increase (two times) of their activities against the microorganisms tested. *S. aureus* was less sensitive than *E. coli* and *C. albicans* to *Gm* and to all new analogues described here, except for c(1–18)[Gln^1]-*Gm*.

As to the assays performed at high salt concentration, only c(1–18)[Gln^1]-*Gm* was as active against *E. coli* as *Gm* at low salt concentration; all other analogues were less active against the microorganism strains studied.

Hemolytic Assay

At 100 μM, *Gm*, [Cys(Acm)^{2,15}]-*Gm* and [Thr^{2,6,11,15},D-Pro^9]-*Gm* was previously described to present the following hemolytic

Table 3. Antimicrobial activities at low and physiological salt concentrations

Peptide nomenclature	MIC (μM)								
	E. coli	R[b]	S[c]	*S. aureus*	R[b]	S[c]	*C. albicans*	R[b]	S[c]
Gm[a]	0.32–0.64	—	2	1.28–2.56	–	2	0.32–0.64	—	4
Gm(2–15)	1.28–2.56	4	2	10.24–20.5	8	2	0.64–1.28	2	8
c(1–18)[Gln^1]-*Gm*	0.32–0.64	1	1	0.64–1.28	0.5	2	0.32–0.64	1	8
[Cys(Acm)^{2,15}]-*Gm*[a]	1.28–2.56	4	2	5.12–10.24	4	8	0.64–1.28	2	8
c(1–18)[Gln^1,Cys(Acm)^{2,15}]-*Gm*	0.64–1.28	2	2	2.56–5.12	2	4	0.64–1.28	2	8
[Thr^{2,6,11,15},D-Pro^9]-*Gm*[a]	1.28–2.56	4	2	5.12–10.24	4	4	0.32–0.64	1	32
c(1–18)[Gln^1,Thr^{2,6,11,15},D-Pro^9]-*Gm*	1.28–2.56	4	2	5.12–10.24	4	2	0.32–0.64	1	32

[a]Peptides used as References [20,21].
[b]R: analogue MIC/gomesin MIC.
[c]S: analogue MIC at 137 mM NaCl/analogue MIC at 86 mM NaCl.

capacities: 40.0%, 16.0% and 17.0%, respectively [24]. These values were confirmed in the present study. For c(1–18)[Gln^{1}]-*Gm*, c(1–18)[Gln^{1},Cys(Acm)^{2,15}]-*Gm* and c(1–18)[Gln^{1},Thr^{2,6,11,15},D-Pro^{9}]-*Gm* at 100 μM they caused 35.5%, 63.0% and 26.5% hemolysis, respectively. The increase observed for c(1–18)[Gln^{1},Cys(Acm)^{2,15}]-*Gm* may be related to the replacement of pGlu^{1} by Gln^{1} required for backbone cyclization as analogue [Gln^{1},Thr^{2,6,11,15},D-Pro^{9}]-*Gm* was as hemolytic as c(1–18)[Gln^{1},Thr^{2,6,11,15},D-Pro^{9}]-*Gm* (data not shown here).

The minimum hemolytic concentrations (capacity to cause 10% or higher hemolysis often used as reference for determination of TI) [21,24] found here for *Gm*, c(1–18)[Gln^{1}]-*Gm*, c(1–18)[Cys(Acm)^{2,15}]-*Gm* and c(1–18)[Gln^{1},Thr^{2,6,11,15},D-Pro^{9}]-*Gm* were 0.39, 0.39, 0.39 and 6.25 μM, respectively.

Serum Stability Assay

Only *Gm* and [Gln^{1},Thr^{2,6,11,15},D-Pro^{9}]-*Gm* as well as their cyclic forms c(1–18)[Gln^{1}]-*Gm* and c(1–18)[Gln^{1},Thr^{2,6,11,15},D-Pro^{9}]-*Gm* were examined in their serum stability. Under the experimental conditions employed, the average percentages of intact peptide found after individual incubation for 6 h in human serum were 87%, 33%, 78% and 28%, respectively.

Circular Dichroism Measurements

Figure 2 shows all the spectra obtained in water, 50% TFE/water and in 50 mM SDS in water. As expected, and similarly to *Gm*, the spectra of c(1–18)[Gln^{1}]-*Gm* in those environments showed a strong negative band around 205 nm and a positive band around 232 nm typical of a β-hairpin structure [21,41] (Figure 2, A1–C1).

In water, the spectrum of the peptide [Cys(Acm)^{2,15}]-*Gm* presented a negative band at about 200 nm expected for unordered structure. Head-to-tail cyclization induced partially folded conformation as indicated by the shoulder around 205 nm in its spectrum. In the presence of SDS or TFE, [Cys(Acm)^{2,15}]-*Gm* and its N/C-cyclized version c(1–18)[Gln^{1},Cys(Acm)^{2,15}]-*Gm* clearly adopted a considerable amount of ordered secondary structure as their spectra have a shape indicative of the presence of β-turns (only a strong negative band around 205 nm) (Figure 2, B1 and C1).

As seen in Figure 2 (B2 and C2), the spectra of [Thr^{2,6,11,1},D-Pro^{9}]-*Gm* and [Gln^{1},Thr^{2,6,11,15},D-Pro^{9}]-*Gm* in 50% TFE/water and 50 mM SDS were coincident to those previously reported by us as they are low intensity α-helix-like spectra, which reveals a tendency for adopting β-hairpin conformations [20]. As to the N/C-cyclized analogue c(1–18)[Gln^{1},Thr^{2,6,11,15},D-Pro^{9}]-*Gm* in 50% TFE/water (Figure 2, B2), it displayed a positive band at 190 nm and two shoulders at about 205 and 215 nm indicative of elements of secondary structure, more specifically representative of type I β-turn [42]. Its spectrum in SDS solution (Figure 2, C2) presented a broad minimum band at 216–220 nm and a positive band between 195 and 200 nm, a pattern proposed by Greenfield and coworkers to be typical of a β-sheet structure [42].

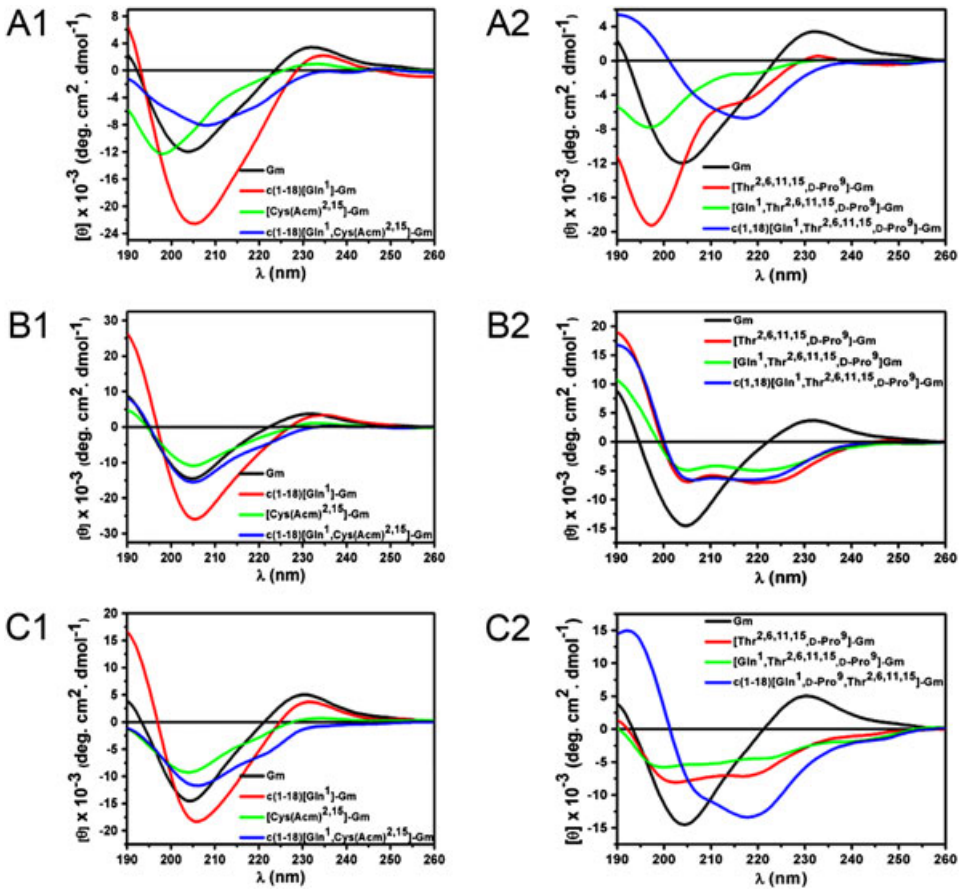

Figure 2. CD spectra of the peptides in water (A), 50 mM SDS in water (B) and 50% TFE/water at pH 4 (C). Peptide concentrations were 20 μM for c(1–18)[Gln^{1}]-*Gm*, c(1–18) [Gln^{1},Cys(Acm)^{2,15}]-*Gm*, [Gln^{1},Thr^{2,6,11,15},D-Pro^{9}]-*Gm* and c(1–18)[Gln^{1}, Thr^{2,6,11,15},D-Pro^{9}]-*Gm* and 100 μM for *Gm*, [Gln^{1},Cys(Acm)^{2,15}]-*Gm* and [Thr^{2,6,11,15},D-Pro^{9}]-*Gm*.

The spectra obtained for *Gm*(2–15) in all environments studied are identical to those of *Gm*, so they are not shown in Figure 2.

Discussion

Optimization of Backbone Cyclization on Resin in at 60 °C

Studies on peptide structure–activity relationship and/or properties of bioactive peptides involving backbone cyclic analogues can be problematic as the synthesis of such complex macromolecules is a challenging task that usually results in very low yield. In this context, choosing the synthetic route can be a real dilemma.

In a preliminary attempt prior to the present study, the total synthesis of c(1–18)[Gln^{1}]-*Gm* was achieved in our laboratory [43]. Hence, the synthetic route initially proposed for making larger amount of it and of the two other cyclic analogues of interest {c(1–18)[Gln^{1},Cys(Acm)^{2,15}]-*Gm* and c(1–18)[Gln^{1}, Thr^{2,6,11,15},D-Pro^{9}]-*Gm*} consisted of the following steps: peptide assembly on resin with Gln^{1} replacing pGlu^{1} peptide detachment from resin/partial side-chain deprotection; if required, disulfide bridge formation; backbone cyclization; purification of the crude peptide; and characterization of the purified peptide. As the analogue c(1–18)[Gln^{1},Cys(Acm)^{2,15}]-*Gm* was the first target of this study, its precursor [Gln^{1},Cys(Acm)^{2,15}]-*Gm* was prepared and characterized by LC/ESI–MS. Detection of unwanted contaminants demanded purification of the crude material prior to conventional backbone cyclization in solution (Figure 3), a very slow reaction at room temperature. Attracted by the possibility of saving time and money, with preservation of quality, and motivated by earlier successful experience of speeding up intramolecular lactam bond formation in CRF analogues linked to MBHA resin at 60 °C [37], we modified the route for the preparation of the two other targets {c(1–18)[Gln^{1}]-*Gm* and c(1–18)[Gln^{1},Thr^{2,6,11,15},D-Pro^{9}]-*Gm*}. Although the new alternative route had an identical number of steps and the final yields were also low, backbone cyclizations occurred on resin (Figure 4**)** and could be notably sped up (30-fold; Table 2) after optimization in 20% DMSO/NMP at 60 °C by using conventional heating and EDC/HOBt.

Such positive impact on the effectiveness of those reactions surely resulted from thermal and diffusion factors. In fact, many authors have shown that chemical reactions needed for stepwise SPPS are significantly accelerated at temperatures higher than 40 °C [44]. In 1997, we reported that at 60 °C, by using conventional heating, manual synthesis of short-sized and middle-sized peptides could be carried out rapidly with maintenance of peptide quality and recovery [45,46]. In the following years, the literature was filled with reports on successful stepwise SPPS at 60 °C or higher temperatures by using conventional heating [29–31] and microwaves [31,47–49], manual microwave-assisted stepwise SPPS using 60 °C as the set temperature [50], microwave-assisted on-bead disulfide bond formation using 60 °C as the set temperature [51] and peptide detachment from resin/full deprotection at 45–50 °C using conventional and microwave heating [52]. As regards to the diffusion factor, it is consensual

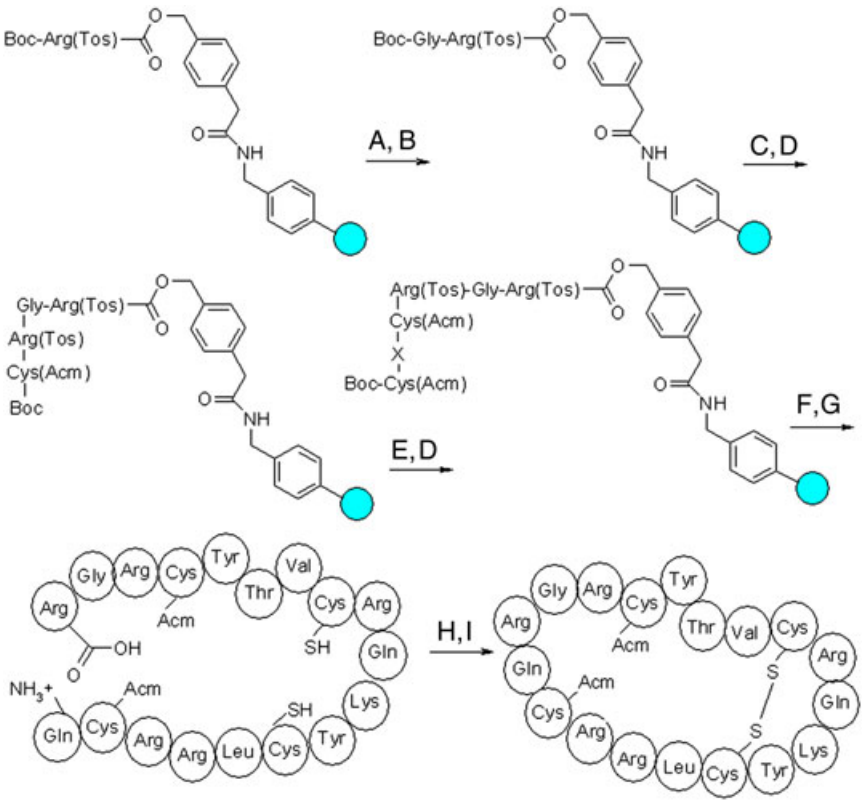

Figure 3. Synthesis of c(1–18)[Gln^{1},Cys(Acm)^{2,15}]-*Gm*. (A) Boc removal: 50% TFA/DCM, 20 min. (B) Boc-Gly–OH coupling: DIC/HOBt (1 : 1, mol/mol) in DCM or TBTU/DIPEA (1 : 3, mol/mol) in DMF, 60 min. (C) Boc removal, Boc-Arg(Tos)–OH coupling. (D) Boc removal, Boc-Cys(Acm)–OH coupling. (E) Boc removal, Boc–amino acid coupling. (F) Boc removal and Boc-Gln–OH coupling. (G) cleavage from resin/full deprotection: HF with anisole/*m*-cresol/DMS [9 : 0.5 : 0.25 : 0.25 (v/v/v/v)], 2 h. (H) Cysteines oxidation: O_2, pH 8.0. (I) Head-to-tail cyclization: EDC/HOBt in DMSO at room temperature. X: Tyr(Bzl), Thr(Bzl), Val, Cys(Meb), Arg(Tos), Gln, Lys(2-Cl-Z), Tyr(Bzl), Cys(Meb), Leu, Arg(Tos), Arg(Tos).

Journal of PeptideScience

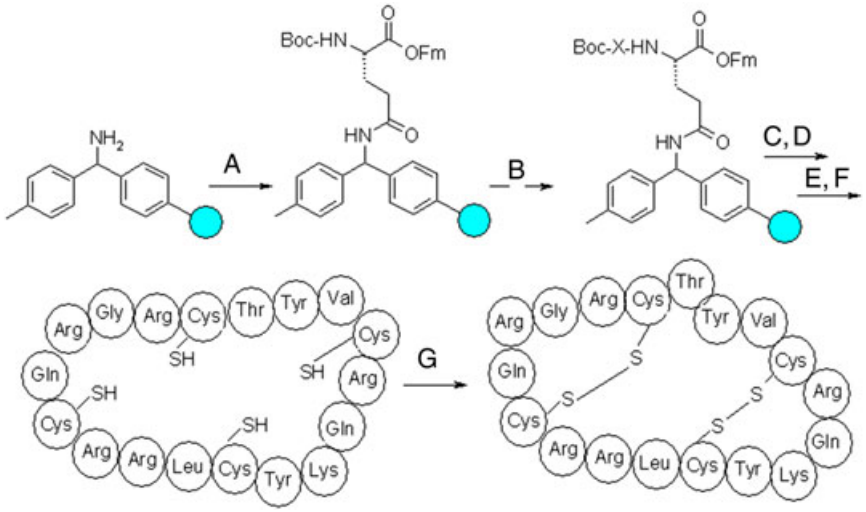

Figure 4. Synthesis of c(1–18)[Gln[1]]-*Gm*. (A) Boc-Glu–OFm coupling: DIC/HOBt (1 : 1, mol/mol) in DCM. (B) Boc removal: 50% TFA/DCM, 20 min followed by Boc–amino acid coupling. (C) Boc removal. (D) Fm removal: 5% DIPEA/DCM, 20% piperidine/DMF, anisole. (E) Head-to-tail cyclization: EDC/HOBt (1 : 1, mol/mol) in 20% DMSO/NMP at 60 °C. (F) Cleavage from resin/full deprotection: HF with anisole/*m*-cresol/DMS [9 : 0.5 : 0.25 : 0.25 (v/v/v/v)], 2 h. (G) Cysteines oxidation: O_2, pH 8.0. X: Arg(Tos), Gly, Arg(Tos), Cys(Meb), Tyr(Bzl), Thr(Bzl), Val, Cys(Meb), Arg(Tos), Gln, Lys(2-Cl-Z), Tyr(Bzl), Cys(Meb), Leu, Arg(Tos), Arg(Tos), Cys(Meb), Gln.

that in traditional SPPS (peptide assembly on resin at room temperature), some solvents and their binary mixtures are able to provide effective swelling of peptide resins, enhancing diffusion of the incoming activated amino acids through their pores and, therefore, facilitating intermolecular and intramolecular chemical reactions [53,54]. The mixture 20% DMSO/NMP, used in the present study and fully stable at 60 °C, is among the binary mixtures of aprotic solvents known to have this capacity, which we could confirm by observing higher solvation degrees of the peptide-MBHA studied than in DMF (data not shown).

It is very important to point out that because high loaded resins, such as the MBHA resin used, yields peptides contaminated by the expected oligomers, chromatography characterization of the linear and cyclic crude products was systematically performed. As they did not contain large amounts of oligomers when analyzed by LC/ESI–MS, it seemed that appropriate dilutions were employed. Anyway, such byproducts were removed by RP-HPLC, negatively affecting the overall yields. As to amino acid enantiomerization during backbone cyclization, EDC/HOBt was mostly used (combination of coupling agent/additive that usually minimizes this side reaction at room temperature [31]). Even so, the diastereoisomers formed were separated by RP-HPLC during the purification step, leading to highly homogeneous final products although at low yields.

It is also relevant to note that our results on cyclizations of [Glu(MBHA resin)[9]]-*Gm* and [Glu(MBHA resin)[1],Thr[2,6,11,15],D-Pro[9]]-*Gm* at room temperature (which required 3 and 2 h, respectively, to give negative Kaiser test [33]) confirmed previous observations that the presence of turn-inducing amino acids, such as D-stereoisomers or N-substituted amino acids, is expected to enhance the rate of the reaction as it stabilizes a cyclization-prone conformation [55,56]. The literature contains reports on microwave-assisted backbone peptide cyclization in solution by native chemical ligation that involves previous synthesis of a protected peptide thioesters [57], peptide cyclizations on resin at room temperature [58], a combination of backbone cyclization and a photocleavable amino acid to give a linear peptide as product [59] and backbone cyclization involving the conversion of the linear peptides into their 4-nitrophenyl esters or other C-terminally activated forms [60]. Nevertheless, to our knowledge, this is the first report of backbone cyclization of a peptide γGlu-linked-MBHA resin at 60 °C using conventional heating, EDC/HOBt and 20% DMSO/NMP.

Impact of Backbone Cyclization on the Properties of *Gm* and Analogues

As expected, the results of the antimicrobial assays and peptide conformational analyses provided complementary information on SAR of *Gm*. Antifungal activities of the new analogue *Gm*(2–15), lacking pGlu[1] and fragment Arg[16]-Glu-Arg[18]-NH_2, revealed that this is not the minimum active portion of *Gm* molecule, results that are in agreement with our previous findings that *Gm* is a highly rigid amphiphatic molecule whose (i) hydrophobic face comprise Leu[5], Tyr[7], Val[12] and Tyr[14]; (ii) hydrophilic face contains Arg[3], Arg[4], Lys[8], Gln[9], Arg[10], Arg[16] and Arg[18]; and (iii) pGlu[1] and Arg[16] are involved in one of the eight hydrogen bonds involved in the high rigidity of the molecule, i.e. the hydrogen bond at the end of one of the β-sheets [18,19]. Therefore, with the help of the truncated analogue *Gm*(2–15), we found in the present study a strong indication that, once bound to a conformationally stabilized folded structure, the N-terminal amino acid pGlu[1] and the amidated C-terminal tripeptide Arg[16]-Glu-Arg[18]-NH_2 play a major role in the interaction of *Gm* with cell membranes of the microorganisms studied, particularly for bacteria. Additional support for such conclusion could be found (i) in the comparative CD spectra of *Gm*(2–15) and *Gm* as they are identical in water, 50% TFE/water and 50 mM SDS in water (for this reason not shown in Figure 2) and (ii) in the results obtained for [Cys(Acm)[2,15]]-*Gm* and [Thr[2,6,11,15],D-Pro[9]]-*Gm* (these other compounds do not contain the C-terminal amide: c(1–18)[Gln[1],Cys(Acm)[2,15]]-*Gm* and c(1–18)[Gln,Thr[2,6,11,15],D-Pro[9]]*Gm*), which contain pGlu[1] and Arg[16]-Glu-Arg[18]-NH_2, but do not acquire a β-hairpin amphiphatic structure in the three environments studied.

Like protegrin and tachyplesin [25,61], *Gm* has two disulfide bridges essential for its full antimicrobial activity and responsible

for its structural rigidity [18,21,62]. The imposition of an additional constraint through backbone cyclization would result in a tricycle that, besides being able to provide new information on SAR of *Gm*, could present improved properties, such as potency, selectivity, salt resistance and/or serum stability. With regard to the antimicrobial activity, we found interesting results because at low salt concentration and pHs used for the biological assays, (i) c(1–18)[Gln^1]-*Gm* has the same nominal net charge of *Gm*, was equipotent against *E. coli* and *C. albicans*, but more active than *Gm* against *S. aureus*; (ii) c(1–18)[Gln^1,$Cys(Acm)^{2,15}$]-*Gm* has the same nominal net charge of [$Cys(Acm)^{2,15}$]-*Gm*, was equipotent against *C. albicans*, but more active against *E. coli* and/or *S. aureus*; (iii) c(1–18)[Gln^1,$Thr^{2,6,11,15}$,D-Pro^9]-*Gm*, a much more simple cyclic analogue to prepare than c(1–18)[Gln^1]-*Gm*, has the same nominal net charge of [$Thr^{2,6,11,15}$,D-Pro^9]-*Gm*, was as potent against all microorganisms tested, but equipotent to *Gm* against *C. albicans*. In other words, as also observed by other authors [25,26], backbone cyclization did not affect or had small effect on the antimicrobial activity of *Gm* and of its monodisulfide and linear analogues previously developed in our laboratories [18]. However, it affected their selectivity.

In terms of low tolerance to high ionic strength, this is a general concern among those studying AMPs and/or aspiring to use them for therapeutic applications. According to many authors, the reduction of antimicrobial activity in high salt concentrations (100–150 mM NaCl) is related to the degree of positive charge of the peptide (which defines its electrostatic attraction for the negatively charged structures of the target cell) to its conformational stability in the physiological conditions and to the target microorganism [25,63]. As highly constrained AMPs found in nature retain their antimicrobial activities under physiological conditions (high salt concentrations) [61], it was logical to investigate whether an AMP can be modified by introducing structural constraints in a manner that it retains its activity with increased salt tolerance. Our *S* values (MIC at 137 mM NaCl/MIC at 86 mM NaCl) indicated that the backbone cyclization increased salt resistance of *Gm* when tested against *E. coli*, an effect not observed in the two cyclic analogues. On the other hand, higher salt tolerance was observed for c(1–18)[Gln^1,$Cys(Acm)^{2,15}$]-*Gm* and c(1–18)[Gln^1,$Thr^{2,6,11,15}$,D-Pro^9]-*Gm* against *S. aureus*. As the level of positive charges of the peptides did not change due to the insertion of a new amide bond involving Arg^{18} and Gln^1, the differences between the cell membranes of the target microorganisms and degrees of structure rigidity in the portion of the molecules encompassing Arg^{16}-Gly-Arg^{18}-Gln^1, as shown by the CD results, may be responsible for such positive differences. Indeed, in the presence of 50 mM SDS, widely used as a simple biomimetic membrane system [32], c(1–18)[Gln^1]-*Gm*, c(1–18)[Gln^1,$Cys(Acm)^{2,15}$]-*Gm* and c(1–18)[Gln^1,$Thr^{2,6,11,15}$,D-Pro^9]-*Gm* presented differences in their conformational stabilities (acquisition of typical β-hairpin structure, considerable amount of ordered secondary structure and β-sheet structure, respectively).

Finally, the observation that the replacement of $pGlu^1$ by Gln^1 and backbone cyclization of *Gm* and of its linearized analogue to give c(1–18)[Gln^1]-*Gm* and c(1–18)[Gln^1,$Thr^{2,6,11,15}$,D-Pro^9]-*Gm* practically did not affect the stability in human serum up to 6 h, clearly revealing that the peptide sites scissible by endoproteases present in such biological environment were not significantly modified, a fact that means that their conformations were fully preserved.

The TI being a key parameter for evaluating if a peptide and its analogues can potentially serve as a lead compound for antimicrobial therapy (the bigger the value, the better the agent and the less toxic it is to the host [21]), the results obtained in the present study show that, against our expectations supported by previous works with protegrin [25,26], no improvement was found with backbone cyclization of *Gm*. Indeed, the TIs for the analogue c(1–18)[Gln^1]-*Gm* are practically identical to those calculated for such potent β-hairpin AMP: 0.60 for *E. coli* and *C. albicans*; 0.30 for *S. aureus*. On the other hand, because of a strong hemolytic activity probably related to higher structural rigidity of the cyclic molecules as indicated by the CD results, considerable TI decrease was observed for c(1–18)[Gln^1,$Cys(Acm)^{2,15}$]-*Gm* and c(1–18)[Gln^1,$Thr^{2,6,11,15}$,D-Pro^9]-*Gm* (values of 0.30 and 2.44 for *E. coli*; 0.07 and 0.006 for *S. aureus*; and 0.30 and 9.76 for *C. albicans*, respectively). Taking all these together, one can deduce that in terms of synthesis cost, antimicrobial activity, hemolytic activity and, therefore, TIs, [$Thr^{2,6,11,15}$,D-Pro^9]-*Gm* (TI of 4.88 for *E. coli*; 1.22 for *S. aureus*; 19.53 for *C. albicans* at low salt concentration [21]) is the most promising active analogue of *Gm* developed in our laboratories. However, its elevated instability in human serum must be overcome.

Conclusions

This study expands the knowledge on the synthesis of structurally complex cyclic peptides, on the effect of backbone cyclization on the properties of biologically active peptides and on SAR of *Gm*. Indeed, we have shown that (i) head-to-tail cyclization of a peptide-polystyrene-based resin can be exceptionally abbreviated using EDC/HOBt as coupling reagents, 20% DMSO/NMP as solvent, 60 °C and conventional heating; (ii) the N-terminal $pGlu^1$ and the amidated C-terminal tripeptide (Arg^{16}-Glu-Arg^{18}-NH_2) are not essential for the β-hairpin amphiphatic structure of *Gm*, but they are critical for *Gm* antimicrobial activity; (iii) except for *Gm*, the replacement of $pGlu^1$ by Gln^1 followed by head-to-tail cyclization had no effect on the activity against *E. coli* and *C. albicans*; (iv) such change increased activity against *S. aureus* and enhanced salt resistance for *E. coli* and salt-sensitivity for *C. albicans*; (v) it practically did not affect serum stability *Gm* and [Gln^1,$Thr^{2,6,11,15}$,D-Pro^9]-*Gm* and had no effect or enhanced their activity on human erythrocytes.

Acknowledgements

This work was supported by grants from FAPESP (Fundação de Amparo à Pesquisa do Estado de São Paulo; 00/05410-2, 01/11296-0, 08/11695-1) to M. T. Machini and post-doctoral fellowship to A. Machado (01/02270-8). The authors thank Dr Cesar Remuzgo for the illustrations.

References

1 Nakamura T, Takahashi H. Epidemiology study of *Candida* infections in blood: susceptibilities of *Candida* spp. to antifungal agents, and clinical features associated with the candidemia. *J. Infect. Chemother.* 2006; **12**: 132–138.
2 Hancock, REW. Cationic peptides: effectors in innate immunity and novel antimicrobials. *Lancet Infect. Dis.* 2001; **1**: 156–164.
3 Jenssen H, Hamill P, Hancock REW. Peptide antimicrobial agents. *Clin. Microbiol. Rev.* 2006; **19**: 491–511.
4 Murakami T, Niwa M, Tokumaga F, Miyata T, Iwanaga S. Direct virus inactivation of tachyplesin I and its isopeptides from horseshoe crab hemocytes. *Chemotherapy* 1991; **37**: 327–334.
5 Morimoto M, Mori H, Otake T, Ueba N, Kumita N, Niwa M, Murakami T, Urakami T, Rakami T, Iwanaga S. Inhibitory effect of tachyplesin-I on

the proliferation of human immunodeficiency virus in vitro. *Chemotherapy* 1991; **37**: 206–211.
6 Masuda M, Nakashima H, Ueda T, Naba H, Ikoma R, Otaka A, Terakawa Y, Tamamura H, Ibuka T, Murakami T, Koyanagi Y, Waki M, Matsumoto A, Yamamoto N, Funakoshi S, Fujii N. A novel anti-HIV synthetic peptide, T-22 ([Tyr^{5,12},Lys^{7}]-polyphemusin II). *Biochem. Biophys. Res. Commun.* 1992; **189**: 845–850.
7 Johnstone SA, Gelmon K, Mayer LD, Hancock REW, Bally MB. *In vitro* characterization of the anticancer activity of membrane-active cationic peptides. I. Peptide-mediated cytotoxicity and peptide-enhanced cytotoxic activity of doxorubicin against wild-type and *p*-glycoprotein over-expressing tumor cell lines. *Anticancer Drug Des.* 2000; **15**: 151–160.
8 Baker MA, Maloy WL, Zasloff M, Jacob LS. Anticancer efficacy of magainin 2 and analogue peptides. *Cancer Res.* 1993; **53**: 3052–3057.
9 Gallo RL, Ono M, Povsic T, Page C, Eriksson E, Klagsbrun M, Bernfield M. Syndecans, cell surface heparan sulfate proteoglycans, are induced by a proline-rich antimicrobial peptide from wounds. *Proc. Natl. Acad. Sci. U. S. A.* 1994; **91**: 11035–11039.
10 Bowdish, DME, Hancock REW. Anti-endotoxin properties of cationic host defence peptides and protein. *J. Endotoxin Res.* 2005; **11**: 230–236.
11 Jenssen H, Hilpert K, Hancock REW. Antibacterial host defence peptides of bovine origin. *Trends Biotechnol.* 1998; **16**: 82–88.
12 Yeaman MR, Yount NY. Mechanisms of antimicrobial peptide action and resistance. *Pharmacol. Rev.* 2003; **55**: 27–55.
13 Bulet P, Stöcklin R, Menin L. Anti-microbial peptides: from invertebrates to vertebrates. *Immunol. Rev.* 2004; **198**: 169–184.
14 Silva Jr. PI, Daffre S, Bulet P. Isolation and characterization of gomesin, an 18-residue cysteine-rich defense peptide from the spider *Acanthoscurria gomesiana* hemocytes with sequence similarities to horseshoe crab antimicrobial peptides of the tachyplesin family. *J. Biol. Chem.* 2000; **275**: 33464–33470.
15 Schaeffer M, de Miranda A, Mottram JC, Coombs GH. Differentiation of *Leishmania major* is impaired by over-expression of pyroglutamyl peptidase I. *Mol. Biochem. Parasitol.* 2006; **150**: 318–329.
16 Moreira CK, Rodrigues FG, Ghosh A, Varotti FP, Miranda A, Daffre S, Jacobs-Lorena M, Moreira LA. Effect of the antimicrobial peptide gomesin against different life stages of *Plasmodium spp*. *Exp. Parasitol.* 2007; **116**: 346–353.
17 Barbosa FM, Daffre S, Maldonado RA, Miranda A, Nimrichter L, Rodrigues ML. Gomesin, a peptide produced by the spider *Acanthoscurria gomesiana*, is a potent anticryptococcal agent that acts in synergism with fluconazole. *FEMS Microbiol. Lett.* 2007; **274**: 279–286.
18 Miranda A, Miranda MTM, Jouvensal L, Volvelle F, Bulet P, Daffre S. Gomesin: a powerful antimicrobial peptide isolated from the Brazilian tarantula spider *Acanthoscurria gomesiana*. In: *Animal Toxins: State of the art. Perspectives in Health and Biotechnology*, Lima MH, Pimenta AMC, Martin-Eauclaire MF (eds). Editora UFMG: Belo Horizonte, 2009; 323–343.
19 Mandard N, Bulet P, Caille A, Daffre S, Vovelle F. The solution structure of gomesin, an antimicrobial cysteine-rich peptide from the spider. *Eur. J. Biochem.* 2002; **269**: 1190–1198.
20 Fázio MA, Oliveira VX, Bulet P, Miranda MTM, Daffre S, Miranda A. Structure-activity relationship studies of gomesin: importance of the disulfide bridges for conformation, bioactivities, and serum stability. *Biopolymers* 2006; **84**: 205–218.
21 Fázio MA, Jouvensal L, Vovelle F, Bulet P, Miranda MTM, Daffre S, Miranda A. Biological and structural characterization of new linear gomesin analogues with improved therapeutic indices. *Biopolymers* 2007; **88**: 386–400.
22 Jelokhani-Niaraki M, Kondejewski LH, Wheaton LC, Hodges RS. Effect of ring size on conformation and biological activity of cyclic cationic antimicrobial peptides. *J. Med. Chem.* 2009; **52**: 2090–2097.
23 Yu Q, Lehrer RI, Tam JP. Engineered salt-insensitive α-defensins with end-to-end circularized structures. *J. Biol. Chem.* 2000; **275**: 3943–3949.
24 Dathe M, Nikolenko H, Klose J, Bienert M. Cyclization increases the antimicrobial activity and selectivity of arginine- and tryptophan-containing hexapeptides. *Biochemistry* 2004; **43**: 9140–9150.
25 Tam JP, Wu CW, Yang JL. Membranolytic selectivity of cystine-stabilized cyclic protegrins. *Eur. J. Biochem.* 2000; **267**: 3289–3300.
26 Kondejewski LH, Farmer SW, Wishart DS, Kay CM, Hancock REW, Hodges RS. Modulation of structure and antibacterial and hemolytic activity by ring size in cyclic gramicidin S analogs. *J. Biol. Chem.* 1996; **271**: 25261–25268.
27 Monroc S, Badosa EFL, Planas M, Montesinos E, Bardaji E. De novo designed cyclic cationic peptides as inhibitors of plant pathogenic bacteria. *Peptides* 2006; **27**: 2567–2574.
28 Moroder L, Musiol H-J, Schaschke N, Chen L, Hargittai B, Barany G. Thiol group. In: *Houben-Weyl, Methods of Organic Chemistry, Synthesis of Peptides and Peptidomimetics*, Goodman M, Felix A, Moroder L, Toniolo C (eds.). E 22a, Georg Thieme Verlag: Stuttgart, 2002; 384–423.
29 Souza MP, Tavares MFM, Miranda MTM. Racemization in stepwise solid-phase peptide synthesis at elevated temperature. *Tetrahedron* 2004; **60**: 4671–4681.
30 Remuzgo C, Andrade GFS, Temperini MLA, Miranda MTM. *Acanthoscurrin* fragment 101–132: total synthesis at 60 °C of a novel difficult sequence. *Biopolymers* 2009; **92**: 65–75.
31 Loffredo C, Assunção NA, Gerhardt J, Miranda MTM. Microwave-assisted solid phase peptide synthesis at 60 °C: alternative conditions with low enantiomerization. *J. Pept. Sci.* 2009; **15**, 808–817.
32 Machado A, Sforça ML, Miranda A, Daffre S, Pertinhez TA, Spisni A, Miranda MTM. Truncation of amidated fragment 33–61 of bovine α-hemoglobin: effects on the structure and anticandidal activity. *Biopolymers* 2007; **88**: 413–426.
33 Kaiser E, Colescott RL, Bossinger CD, Cook PI. Color test for the detection of free terminal amino groups in the solid-phase synthesis of peptides. *Anal. Biochem.* 1970; **34**: 595–598.
34 Trzeciak A, Bannwarth W. Synthesis of 'head-to-tail' cyclized peptides on solid support by Fmoc chemistry. *Tetrahedron Lett.* 1992; **33**: 4557–4560.
35 McMurray JS. Solid phase synthesis of a cyclic peptide using Fmoc chemistry. *Tetrahedron Lett.* 1991; **32**: 7679–7682.
36 Rovero P, Quartara L, Fabbri G. Synthesis of cyclic peptides on solid support. *Tetrahedron Lett.* 1991; **32**: 2639–2642.
37 Machado A, Xavier GC, Miranda A, Miranda MTM. Lactam bridge formation at high temperature. In *Peptide Revolution: Genomics, Proteomics & Therapeutics* (Proc. 18th. Am. Pept. Symp.) Chorev M, Sawyer TK (eds). American Peptide Society: San Diego, 2004; 192–193.
38 Mant CT, Hodges, RS. *High-Performance Liquid Chromatography of Peptides and Proteins: Separation, Analysis and Conformation*. CRC Press Inc: Boca Raton, 1991.
39 Fehlbaum P, Bulet P, Michaut L, Lagueux M, Broekaert WF, Hetru C, Hoffmann JA. Insect immunity. Septic injury of *Drosophila* induces the synthesis of a potent antifungal peptide with sequence homology to plant antifungal peptides. *J. Biol. Chem.* 1994; **269**: 33159–33163.
40 Bulet P, Dimarcq JL, Hetru C, Lagueux M, Charlet M, Hegy G, Van Dorsselaer A, Hoffmann JA. A novel inducible antibacterial peptide of *Drosophila* carries an *O*-glycosylated substitution. *J. Biol. Chem.* 1993; **268**: 14893–14897.
41 Perczel A, Hollósi M, Foxman BM, Fasman GD. Conformational analysis of pseudocyclic hexapeptides based on quantitative circular dichroism (CD), NOE, and X-ray data. The pure CD spectra of type I and II β-turns. *J. Am. Chem. Soc.* 1991; **113**: 9772–9784.
42 Greenfield NJ, Fasman GD. Computed circular dichroism spectra for the evaluation of protein conformation. *Biochemistry* 1969; **8**: 4108–4116.
43 Machado A, Fázio, MA, Miranda A, Daffre S, Miranda MTM. Synthesis of conformationally constrained head-to-tail cyclic gomesin. In: *Peptides 2002* (Proc. 27th. Eur. Pept. Symp.), Benedetti E., Pedone C (eds.). Edizione Ziino: Napoli, Italy, 2002; 224–225. Abstract published in *J. Pept. Sci*., 2002; **8**: S88 (PA44).
44 Rabinovich AK, Rivier JE. In *Peptides: Chemistry, Structure and Biology* (Proc. 13th. Am. Pept. Symp.), Hodges RS, Smith JA (eds.). Escom Science Publishers BV: Leiden, The Netherlands, 1994; 71–73.
45 Varanda LM, Miranda MTM. Solid-phase peptide synthesis at elevated temperature: a search for an optimized synthesis condition of unsulfated cholecystokinin-12. *J. Pept. Res.* 1997; **50**: 102–108.
46 Rivier JE, Miranda MTM. Solid-phase peptide synthesis at elevated temperature. In: *Synthesis of Peptides and Peptidomimetics*, vol. E22a, Goodman M, Felix A, Moroder L, Toniolo C (eds.). Thieme: Stuttgart, 2002; 806–813.
47 Rizzolo F, Sabatino G, Chelli M, Rovero P, Papini AM. A convenient microwave-enhanced solid-phase synthesis of difficult peptide sequences: case study of gramicidin A and CSF114(Glc). *Int. J. Pept. Protein Chem. Bio.* 2007; **13**: 203–208.
48 Sabatino G, Papini AM. Advances in automatic, manual and microwave-assisted solid-phase peptide synthesis. *Curr. Opin. Drug Discov. Devel.* 2008; **11**: 762–770.

49 Bacsa B, Desai B, Gábar D, Kappe CO. Rapid solid-phase peptide synthesis using thermal and controlled microwave irradiation. *J. Pept. Sci.* 2006; **12**: 633–638.
50 Bacsa B, Horváti K, Bosze S, Andreae F, Kappe CO. Solid-phase synthesis of difficult peptide sequences at elevated temperatures: a critical comparison of microwave and conventional heating technologies. *J. Org. Chem.* 2008; **73**: 7532–7542.
51 Galanis AS, Albericio F, Grotli M. Enhanced microwave assisted on-bead disulfide bond formation method. Synthesis of alpha-conotoxin MII. *J. Pept. Sci.* 2008; **14**: 73–74.
52 Kluczyk A, Rudowska M, Stefanowicz P, Szewczuk Z. Microwave-assisted TFA cleavage of peptides from Merrifield resin. *J. Pept. Sci.* 2009; **16**: 31–39.
53 Oliveira, E; Cilli, EM; Miranda, A, Jubilut GN, Albericio F, Andreu D, Paiva ACM, Schreier S, Tominaga M, Nakaie CR. Monitoring the chemical assembly of a transmembrane bradykinin receptor fragment: correlation between resin solvation, peptide chain mobility, and rate of coupling. *Eur. J. Org. Chem.* 2002; **2002**: 3686–3694.
54 Alcaro MC, Sabatino G, Uziel J, Chelli M, Ginanneschi M, Rovero P, Papini AM. On-resin head-to-tail cyclization of cyclotetrapeptides: optimization of crucial parameters. *J. Pept. Sci.* 2004; **10**: 218–228.
55 Page K, Hood CA, Patel H, Fuentes G, Menakuru M, Park JH. Fast Fmoc synthesis of hAmylin(1–37) with pseudoproline assisted on-resin disulfide formation. *J. Pept. Sci.* 2007; **13**: 833–838.
56 Klose, J, Ehrlich, A, Bienert, M. Infuence of proline and β-turn mimetics on the cyclization of penta- and hexapeptides. *Lett. Pept. Sci.* 1998; **5**: 129–131.
57 Park S, Gunasekera S, Leta Aboye T, Göransson U. An efficient approach for the total synthesis of cyclotides by microwave assisted Fmoc-SPPS. *Int. J. Pept. Res. Ther.* 2010; **16**: 167–176.
58 Ovadia O, Linde Y, Haskell-Luevano C, Dirain ML, Sheynis T, Jelinek R, Gilon C, Hoffman A. The effect of backbone cyclization on PK/PD properties of bioactive peptide-peptoid hybrids: the melanocortin agonist paradigm. *Bioorg. Med. Chem.* 2010; **18**: 580–589.
59 Umezawa N, Noro Y, Ukai K, Katao N, Higuchi T. Photocontrol of peptide function: backbone cyclization strategy with photocleavable amino acid. *Chembiochem*, 2011; **12**: 1694–1698.
60 Davies JS. The cyclization of peptides and depsipeptides. *J. Pept. Sci.* 2003; **9**: 471–501.
61 Harwig SSL, Waring A, Yang HJ, Cho Y, Tan L, Lehrer RI. Intramolecular disulfide bonds enhance the antimicrobial and lytic activities of protegrins at physiological sodium chloride concentrations. *Eur. J. Biohem.* 1996; **240**: 352–357.
62 Bolintineanu DS, Langham, AA, Davis HT, Kaznessis YN. Molecular dynamics simulations of free protegrin-type antimicrobial peptides: interplay between charges at the termini, β-sheet structure and amphiphilic interactions. *Mol. Simul.* 2007; **33**: 809–819.
63 Yenugu S, Hamil KG, Birse CE, Ruben SM, French FS, Hall SH. Antibacterial properties of the sperm-binding proteins and peptides of human epididymis 2 (HE2) family; salt sensitivity, structural dependence and their interaction with outer and cytoplasmic membranes of *Escherichia coli*. *Biochem. J.* 2003; **372**: 473–483.

